

Deflection angle and Shadows by Black Holes in Starobinsky-Bel-Robinson Gravity from M-theory

A. Belhaj^{1*}, H. Belmahi^{1†}, M. Benali^{1‡}, Y. Hassouni^{1§}, M. B. Sedra^{2 ¶}

¹ Département de Physique, Equipe des Sciences de la matière et du rayonnement, ESMaR

Faculté des Sciences, Université Mohammed V de Rabat, Rabat, Morocco

² Material and subatomic physics laboratory, LPMS, University of Ibn Tofail, Kenitra, Morocco

April 11, 2023

Abstract

Motivated by M-theory compactifications, we investigate optical properties of black holes in the Starobinsky-Bel-Robinson gravity. Precisely, we study the shadows and the deflection angle of light rays by non-rotating and rotating black holes in such a novel gravity. We start by discussing the shadows of the Schwarzschild-type solutions. As expected, we obtain perfect circular shadows where the size decreases with a stringy gravity parameter denoted by β . We show that this parameter is constrained by the shadow existence. Combining the Newman-Janis algorithm and the Hamilton-Jacobi mechanism, we examine the shadow behaviors of the rotating solutions in terms of one-dimensional real curves. Essentially, we find various sizes and shapes depending on the rotating parameter and the stringy gravity parameter a and β , respectively. To inspect the shadow geometric deformations, we investigate the astronomical observables and the energy emission rate. As envisaged, we reveal that a and β have an impact on such shadow behaviors. For specific values of a , we remark that the obtained shadow shapes share certain similarities with the ones of the Kerr black holes in plasma backgrounds. Using the Event Horizon Telescope observational data, we provide predictions for the stringy gravity parameter β which could play a relevant role in M-theory compactifications. We finish this work by a discussion on the behaviors of the light rays near to such four dimensional black holes by computing the deflection angle in terms of a required moduli space.

*a-belhaj@um5r.ac.ma

†hajar_belmahi@um5.ac.ma

‡mohamed_benali4@um5.ac.ma

§y.hassouni@um5r.ac.ma

¶Authors in alphabetical order.

Contents

1	Introduction	3
2	Black holes in SBR gravity	5
3	Shadows of SBR black holes	6
3.1	Shadows of non-rotating SBR black holes	7
3.2	Shadow behaviors of rotating SBR black holes	10
3.2.1	Shadows of rotating SBR black holes	10
3.2.2	Geometric deformations of the shadow	12
3.2.3	Energy emission rate	14
3.2.4	Constraints on the stringy gravity parameter via EHT observational data	15
4	Light ray behaviors near to SBR black holes	16
4.1	Deflection angle of non-rotating solutions	18
4.2	Deflection angle of rotating SBR black holes	19
5	Conclusion	21

1 Introduction

The study of black hole physics becomes a warm subject approached from different gravity theories including the modified ones. This relevant interest has been supported and encouraged by the observational results brought either by Event Horizon Telescope (EHT) collaborations or by the gravitational wave detections [1–4]. These physical activities are behind the most recent development dealing with various black hole properties including the thermodynamic and the optical ones. These properties have been largely investigated by considering certain gravity models living in different background geometries such as the Anti-Sitter space-times (AdS) [5, 6]. These non-trivial geometries open gates to approach the thermodynamic aspect by identifying the cosmological constant with the pressure [7–9]. This identification has been explored to investigate the thermodynamic behaviors such as the stability and the phase transitions of many black holes in arbitrary dimensional gravity theories including supergravity ones like Type II superstrings and M-theory scenarios [10–15]. In this context, several thermodynamic quantities have been computed and examined. The entropy, the heat capacity and the Gibbs free energy have been calculated, being needed to study local and global stabilities. They have been exploited also in the discussion of the Hawking-Page transition between a large stable black hole and a thermal gas in AdS geometries using analytical and numerical methods. Using the result of the AdS/CFT conjecture, the thermodynamics and the thermodynamical geometry of the AdS black holes from M-theory in the presence of M2 and M5-branes with and without dark energy have been investigated [16]. Concretely, the stability and the phase transitions of four and seven dimensional AdS black holes have been studied in terms of the M-brane number.

Parallely, the optical properties of the black holes have been largely investigated using analytical and numerical approaches. A close examination shows that two relevant concepts have been studied being the shadow and the deflection angle of the light rays near to black holes [17–27]. The first concept has been obtained via the Hamilton-Jacobi algorithm providing the equations of motion of photons near to a black hole solution [28, 29]. In four dimensions, for instance, the shadow behaviors have been approached in terms of one-dimensional closed real curves. The size and the shape of such curves depend on the moduli space of the black hole in question. Precisely, the non-rotating black hole involves perfect circular shadows where the size could be controlled by certain parameters such as the charge. The spin parameter, however, affects such geometries by providing distortion deformations leading to non-trivial configurations known as D-shapes [30–34]. Among others, the shadows of four-dimensional AdS black holes in M-theory scenarios have been investigated in terms of the M2-brane number. It has been shown that such a number controls the geometric deformation of the shadows [35, 36]. Using the Gauss-Bonnet theorem, moreover, the deflection angle and the trajectory of the light rays near to black holes derived from the compactification of M-theory on the real spheres on S^7 and S^4 have been studied [37]. In particular, the impact of the M-brane number and the rotating parameter on such optical behaviors has been examined.

Recently, modified gravity models, being used to solve certain Universe problems, have been exploited to study black holes. Many theories have been proposed using different roads and methods. Precisely, the most studied one is Einstein Gauss-Bonnet (EGB) gravity supported by string theory and related dual models including M-theory [38–40]. Black holes in such gravity models have been built and studied in terms of a parameter called Gauss-Bonnet gravity parameter. The thermodynamics and the optical properties of these black holes have been dealt with in terms of such a parameter [41, 42]. It has been shown that the Gauss-Bonnet parameter has a relevant impact on the black hole physical properties [43, 44]. It has been observed that the shadow radius decreases by increasing this parameter [45].

More recently, a novel Starobinsky-Bel-Robinson (SBR) gravity has been constructed by introducing a new stringy parameter called β [46]. This four-dimensional gravity has been inspired by M-theory described, at lower energies, by eleven-dimensional supergravity. Concretely, it has been suggested that this modified gravity could be derived from the compactification of M-theory on a two sphere factor being $S^3 \times S^4$ [46]. Models in such a novel gravity have been proposed. Concretely, inflation scenarios with the stringy gravity parameter β have been treated where the associated cosmological observables have been computed [47]. It has been suggested that the observational data can impose constraints on such a parameter. Moreover, the Schwarzschild-type black holes in the SBR gravity have been built. Precisely, the corresponding thermodynamic properties have been addressed in terms of β by computing the relevant quantities including the entropy and the pressure. An examination reveals that these quantities are corrected by the presence of β [48].

The aim of this work is to contribute to such activities by investigating the optical properties of black holes in the SBR gravity which could be embedded in M-theory scenarios. Particularly, we study the shadows and the deflection angle of light rays by non-rotating and rotating black holes in four dimensions. We start by discussing the shadow of the Schwarzschild-type solutions in such a novel gravity. As expected, we obtain perfect circular configurations where the size decreases with the stringy gravity parameter β being constrained by the shadow existence. Combining the Newman-Janis algorithm and the Hamilton-Jacobi mechanism, we study the shadow behaviors of the rotating solutions in terms of one-dimensional real curves. In the β range, we find various sizes and shapes depending on the rotating and the gravity parameters a and β , respectively. To examine the shadow geometric deformations, we study the astronomical observables and the energy emission rate. As envisaged, we show that the stringy rotating parameter a and the gravity parameter β have a relevant impact on the shadow aspect. For specific values of a , we observe that the derived shadow shapes share certain similarities with the ones of the Kerr black hole in plasma backgrounds [49, 50]. Using the observational EHT data, we provide predictions for β which could play a primordial role in the M-theory compactification. Finally, we discuss the light ray behaviors near to the SBR black holes by calculating and analyzing the deflection angle in terms of the rotating and the stringy gravity parameters.

The organization of this paper is as follows. In section 2, we reconsider the study of the black holes in the SBR gravity. In section 3, we investigate the shadow behaviors and provide

predictions for β by the help of EHT data. In section 4, we analyze the light ray behaviors near to the SBR black holes by computing and analyzing the deflection angle variation. In the last section, we provide concluding remarks.

2 Black holes in SBR gravity

In this section, we give a concise reconsideration on black hole solutions in modified gravity theories originated from higher dimensional space-times. In particular, we deal with certain black hole solutions in the SBR gravity which could be embedded in M-theory living in the eleven dimensional space-time, recently reported in [46]. It is recalled that M-theory involves a specific bosonic sector containing a metric g_{MN} and a tensor 3-form C_{MNP} coupled to M2-branes being dual to M5-branes [51]. The associated four-dimensional gravity models could be obtained using the compactification mechanism with the presence of stringy fluxes required by the stabilization scenarios [46, 48]. Roughly speaking, the action we consider here reads as

$$S_{SBR} = \frac{M_{pl}}{2} \int d^4x \sqrt{-g} \left(R + \frac{R^2}{6m^2} - \frac{\beta}{32m^6} (P_4^2 - E_4^2) \right) \quad (2.1)$$

where g is the determinant of the metric and R is the Ricci curvature. m is a free mass parameter which could have various interpretations depending on the underlying theory. β is a positive dimensionless coupling which will be considered as a relevant parameter in the present investigation. It is worth noting that such a parameter depends on the M-theory compactification which could be fixed from the black hole optical behaviors. P_4^2 and E_4^2 are quartic contributions associated with the Pontryagin and the Euler topological densities. According to [46, 48], the last term is linked to the Bel-Robinson tensor $T_{\mu\nu\lambda\rho}$ in four dimensions by means of the relation

$$T^{\mu\nu\lambda\rho} T_{\mu\nu\lambda\rho} = \frac{1}{4} (P_4^2 - E_4^2) \quad (2.2)$$

where one has used

$$T^{\mu\nu\lambda\sigma} = R^{\mu\rho\gamma\lambda} R_{\rho\gamma}^{\nu\sigma} + R^{\mu\rho\gamma\sigma} R_{\rho\gamma}^{\nu\lambda} - \frac{1}{2} g^{\mu\nu} R^{\rho\gamma\alpha\lambda} R_{\rho\gamma\alpha}^{\sigma}. \quad (2.3)$$

A close inspection reveals that the SBR gravity action involves two parameters m and β . This action has been approached to provide physical models including inflation [47]. Moreover, the Schwarzschild type black holes in such a gravity have been built where the parameter m has been absorbed by solving the associated equation of motion [48]. Concretely, the corresponding thermodynamic quantities have been also computed and investigated. It has been shown that such quantities are corrected by the stringy gravity parameter β . In this way, the line element of this non-rotative solution has been found to be

$$ds^2 = -f(r)dt^2 + \frac{1}{f(r)}dr^2 + r^2d\Omega^2 \quad (2.4)$$

where the fundamental metric function $f(r)$ is given by

$$f(r) = 1 - \frac{r_s}{r} + \beta \left(\frac{4\sqrt{2}\pi Gr_s}{r^3} \right)^3 \left(\frac{108r - 97r_s}{5r} \right) \quad (2.5)$$

where one has used $r_s = 2GM$. Here, G and M represent the Newton constant and the mass parameter, respectively. Having considered the non-rotating case, we could construct the rotating black holes in the SBR gravity. To provide such solutions, it has been suggested an useful algorithm called the Newmann-Janis algorithm [52,53]. A close examination shows that this approach can be adopted for certain modified gravity models by introducing extra parameters. Supported by such activities, we would like to investigate rotating black holes in the SBR gravity. Applying the Boyer-Lindquist coordinate systems, we propose and assume the following metric line element

$$ds^2 = - \left(\frac{\Delta(r) - a^2 \sin^2 \theta}{\Sigma} \right) dt^2 + \frac{\Sigma}{\Delta(r)} dr^2 - 2a \sin^2 \theta \left(1 - \frac{\Delta(r) - a^2 \sin^2 \theta}{\Sigma} \right) dt d\phi + \Sigma d\theta^2 + \sin^2 \theta \left[\Sigma + a^2 \sin^2 \theta \left(2 - \frac{\Delta(r) - a^2 \sin^2 \theta}{\Sigma} \right) \right] d\phi^2 \quad (2.6)$$

where one has used

$$\Delta(r) = a^2 + r^2 \left(1 - \frac{2GM}{r} + \frac{1024\pi^3 \beta G^6 M^3 (108r - 194GM)}{5r^{10}} \right) \quad (2.7)$$

$$\Sigma = r^2 + a^2 \cos^2 \theta. \quad (2.8)$$

This line element contains two parameters a and β recovering quite known solutions. Putting $a = 0$, we obtain the previous non-rotating black holes. Taking $\beta = 0$, however, we recover the Kerr metric associated with the following delta function

$$\Delta_{Kerr}(r) = a^2 + r^2 - 2GM r. \quad (2.9)$$

In what follows, the stringy gravity parameter β will be crucial to inspect the optical behaviors of the SBR black holes going beyond the thermodynamic ones reported in [48]. The aim of the remaining part of this work is to investigate the light behaviors around the SBR black holes.

3 Shadows of SBR black holes

The EHT international collaboration has brought a black hole image which has been considered as a relevant discovery in the underlying physics [1,2]. Indeed, it has been remarked that when the light passes near to a black hole, certain optical behaviors occur. Precisely, the light rays could be deviated quite strongly and could travel via circular geometrical configurations. These considerations support the idea that a black hole can be viewed as a dark disk in the sky. This disk is known by the shadow. Motivated by shadow activities, many black hole solutions have been investigated using different approaches. These

activities open gates to unveil more data on optical behaviors of black holes by studying the relevant concepts being the shadow and the deflection angle of the light rays. These concepts can be dealt with to provide a test of gravity model predictions in the face of the EHT observational data. This empiric exam could fix certain gravity parameters originated from M-theory compactifications.

In this section, we study the shadow cast behavior of black holes in such a SBR gravity. This study will be made in terms of one-dimensional real curves carrying the most data on the involved size and the shape deformations. The present optical behaviors can be approached via the null geodesic equations of motion. To derive such equations, we can adopt the Hamilton-Jacobi algorithm based on the following equation

$$\frac{dS}{d\tau} = -\frac{1}{2}g^{\mu\nu} \frac{dS}{dx^\mu} \frac{dS}{dx^\nu}, \quad (3.1)$$

where τ is the affine parameter. S represents the Jacobi action which can be expressed as follows

$$S = -Et + L\phi + S_r(r) + S_\theta(\theta), \quad (3.2)$$

where E and L correspond to the energy and the momentum of the photon, respectively. They are given by

$$E = -p_t \quad L = -p_\phi. \quad (3.3)$$

S_r and S_θ are functions of r and θ variables, respectively. Using the separation method, the four-dimensional equations of motion can be determined for several black hole solutions including the non-rotating and the rotating ones.

3.1 Shadows of non-rotating SBR black holes

To get the associated shadows, we consider the black hole solutions given by Eq.(2.4). Applying the separation method [28], we get the factorized relations

$$r^2 f(r) \left(\frac{dS_r(r)}{dr} \right)^2 - r^2 \frac{E^2}{f(r)} + L^2 = -\mathcal{K}, \quad (3.4)$$

$$\left(\frac{dS_\theta(\theta)}{d\theta} \right) + L^2 \cot^2 \theta = \mathcal{K}, \quad (3.5)$$

where \mathcal{K} is the Carter constant which can be considered as a motion constant. The equations of motion are given by

$$\frac{dt}{d\tau} = \frac{E}{f(r)} \quad (3.6)$$

$$r^2 \frac{dr}{d\tau} = \pm \sqrt{-r^2 f(r) (\mathcal{K} + L^2) + E^2 r^4} \quad (3.7)$$

$$r^2 \frac{d\theta}{d\tau} = \pm \sqrt{\mathcal{K} - L^2 \cot^2 \theta} \quad (3.8)$$

$$\frac{d\phi}{d\tau} = \frac{L}{r^2 \sin^2 \theta}. \quad (3.9)$$

Using the radial equation, the effective potential takes the following form

$$V_{eff}(r) = - \left(\frac{dr}{d\tau} \right)^2. \quad (3.10)$$

The calculation provides

$$V_{eff}(r) = \frac{f(r)}{r^2} (\mathcal{K} + L^2) - E^2. \quad (3.11)$$

This effective potential should satisfy the following conditions

$$V_{eff}(r) \Big|_{r=r_c} = 0, \quad \frac{dV_{eff}(r)}{dr} \Big|_{r=r_c} = 0 \quad (3.12)$$

where r_c represent the radius of the unstable circular orbits. This radius can be obtained by solving the equation

$$f'(r) - 2f(r) = 0 \quad (3.13)$$

where the prime notation denotes the derivative with respect to the radial coordinate. A close examination shows that the shadow geometries can be established by means of the impact parameters. In four dimensions, these parameters read as

$$\xi_{SBR} = \frac{L}{E} \quad \eta_{SBR} = \frac{\mathcal{K}}{E^2} \quad (3.14)$$

which are given in terms of the conserved quantities. In the non-rotating case, the computations give

$$\xi_{SBR}^2 + \eta_{SBR} = \frac{25r_c^{12}}{1390592\pi^3\beta G^7 M^4 - 663552\pi^3\beta G^6 M^3 r_c - 20GM r_c^9 + 15r_c^{10}} \quad (3.15)$$

generating one-dimensional real curves in a two-dimensional plane. To get a more clear configurations, the celestial coordinates should be exploited. Indeed, they are given by

$$X_{SBR} = \lim_{r_o \rightarrow +\infty} \left(-r_o^2 \sin \theta_o \frac{d\phi}{dr} \right) \quad (3.16)$$

$$Y_{SBR} = \lim_{r_o \rightarrow +\infty} \left(r_o^2 \frac{d\theta}{dr} \right) \quad (3.17)$$

where r_o indicates the distance of the observer from the black hole, while θ_o represents the angle of the inclination between the observer line of sight and the axis of the black hole rotation. In this way, the left-hand side of Eq.(3.15) can be rewritten as follows

$$\xi_{SBR}^2 + \eta_{SBR} = X_{SBR}^2 + Y_{SBR}^2. \quad (3.18)$$

To get the shadow cast representation, we should handle this equation by combining Eq.(3.13) and Eq.(3.15) via a numerical method. Before going ahead, we first inspect the event horizon radius r_+ behaviors in terms of the stringy gravity parameter β . Fig.(1) gives the horizon radius as a function of such a parameter. In certain regions of the moduli space, it follows

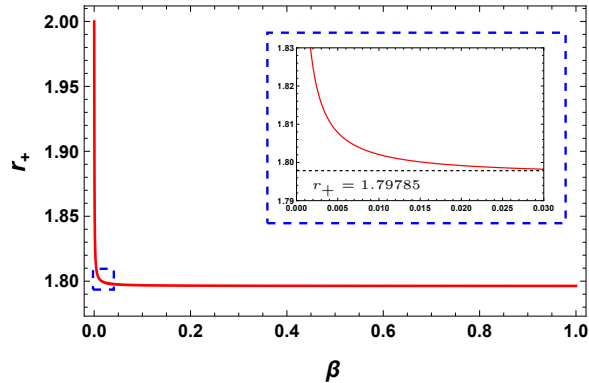


Figure 1: *Horizon size behaviors of SBR black holes by varying the string parameter.*

from this figure that the horizon radius of the SBR black holes decreases by increasing β . For values $\beta \geq 3.10^{-2}$, however, the horizon radius keeps a constant value around $r_+ \simeq 1.798$. Taking into account such constraints, we can now investigate the shadow behaviors of the non-rotating black holes in the SBR gravity by varying the stringy gravity parameter and fixing the above ones namely G and M to 1. Fig.(2) depicts the shadows of the SBR black holes as a function of β . As expected, the obtained shadow geometries are perfect circles. We

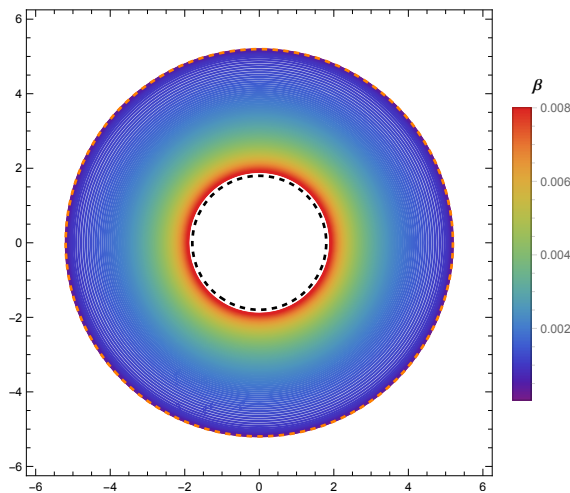


Figure 2: *Shadow behaviors of SBR black by varying the parameter β . The orange and black dashed circle represents the shadow of Schwarzschild and the horizon limite, respectively.*

observe that the stringy gravity parameter β controls their sizes. Precisely, they decrease by increasing β . A close examination on shadow behaviors shows that we should impose extra conditions on β . For $\beta > 8.10^{-2}$, we remark that the radius of the horizon becomes large that the shadow one. This leads to a condition on the shadow existence matching perfectly with the findings associated with the cosmological building models embedded in the SBR gravity [47]. These small values of β can be supported by others investigations [46, 48]. This could provide certain bridges between inflation and black holes built from the SBR gravity.

Having investigated the non-rotating case, we move to consider the implementation of the rotating parameter in the shadow discussions.

3.2 Shadow behaviors of rotating SBR black holes

In this section, we would like to study optical behaviors of the rotating black holes in the SBR gravity. Precisely, we investigate the shadow behaviors in such M-theory inspired black hole models.

3.2.1 Shadows of rotating SBR black holes

Here, we consider the rotating version of the black holes in the SBR gravity. Using the separation method to the metric (2.6), we get

$$\Sigma \frac{dt}{d\tau} = \frac{r^2 + a^2}{\Delta} (E(r^2 + a^2) - aL) - a(aE \sin^2 \theta - L), \quad (3.19)$$

$$\Sigma \frac{dr}{d\tau} = \pm \sqrt{\mathcal{R}(r)}, \quad (3.20)$$

$$\Sigma \frac{d\theta}{d\tau} = \pm \sqrt{\Theta(\theta)}, \quad (3.21)$$

$$\Sigma \frac{d\phi}{d\tau} = \frac{a}{\Delta} (E(r^2 + a^2) - aL) - \left(aE - \frac{L}{\sin^2 \theta} \right), \quad (3.22)$$

where $\mathcal{R}(r)$ and $\Theta(\theta)$ read as

$$\mathcal{R}(r) = ((r^2 + a^2)E - aL)^2 - \Delta((aE - L)^2 + \mathcal{K}), \quad (3.23)$$

$$\Theta(\theta) = \mathcal{K} - \left(\frac{L^2}{\sin^2 \theta} - a^2 E^2 \right) \cos^2 \theta. \quad (3.24)$$

The unstable photon orbits should satisfy the constraints

$$\mathcal{R}(r) \Big|_{r=r_0} = 0, \quad \frac{\partial \mathcal{R}(r)}{\partial r} \Big|_{r=r_0} = 0. \quad (3.25)$$

In the case of the rotating solutions, the impact parameters take the following forms

$$\eta_{SBR} = \frac{r^2 [16\Delta(r)(a^2 - \Delta(r)) - r^2 \Delta'(r)^2 + 8r\Delta(r)\Delta'(r)]}{a^2 \Delta'(r)^2} \Big|_{r=r_0}, \quad (3.26)$$

$$\xi_{SBR} = \frac{(a^2 + r^2)\Delta'(r) - 4r\Delta(r)}{a\Delta'(r)} \Big|_{r=r_0}. \quad (3.27)$$

Using the fact that β is very small, the computations give

$$\eta_{SBR} = \eta_{KR} + \beta\gamma_1 \quad (3.28)$$

$$\xi_{SBR} = \xi_{KR} + \beta\gamma_2 \quad (3.29)$$

where η_{KR} and ξ_{KR} are the impact parameters of the Kerr black hole which read as

$$\eta_{KR} = \frac{r_0^3 (4a^2 GM - r_0(r_0 - 3GM)^2)}{a^2 (r_0 - GM)^2} \quad (3.30)$$

$$\xi_{KR} = \frac{r_0^2 (3GM - r_0) - a^2 (GM + r_0)}{a (r_0 - GM)}. \quad (3.31)$$

γ_1 and γ_2 are two independent functions of β given by

$$\begin{aligned} \gamma_1 &= 8192\pi^3 G^6 M^3 \left[\frac{(a^2 (1261G^2 M^2 - 1106GM r_0 + 243r_0^2))}{5a^2 r_0^6 (r_0 - GM)^3} \right. \\ &\quad \left. + \frac{r_0 (-2619G^3 M^3 + 3624G^2 M^2 r_0 - 1646GM r_0^2 + 243r_0^3)}{5a^2 r_0^6 (r_0 - GM)^3} \right] \quad (3.32) \\ \gamma_2 &= \frac{4096\pi^3 G^6 M^3 (a^2 (388GM - 189r_0) + r_0 (-873G^2 M^2 + 917GM r_0 - 243r_0^2))}{5ar_0^8 (r_0 - GM)^2}. \end{aligned}$$

It is denoted that the impact parameters of the SBR black holes depend on β and the ones of the Kerr black hole. For $\beta = 0$, such impact parameters reduce to the Kerr ones. As envisaged, β could affect the geometry of the shadows by means of the size and the shape. According to [28, 29], the coordinates of a celestial plane (X_{SBR}, Y_{SBR}) representing all projections of the spherical photon orbits will be exploited in the computations. Indeed, they are given by

$$X_{SBR} = -r_o \frac{p^{(\phi)}}{p^{(t)}} = \lim_{r_o \rightarrow \infty} \left(-r_o^2 \sin \theta_o \frac{d\phi}{dr} \right), \quad (3.33)$$

$$Y_{SBR} = r_o \frac{p^{(\theta)}}{p^{(t)}} = \lim_{r_o \rightarrow \infty} \left(r_o^2 \frac{d\theta}{dr} \right) \quad (3.34)$$

where r_o and θ_o denote the distance and the angle of the observer, respectively. Such celestial coordinates and the above impact parameters are linked via the following relations

$$X_{SBR} = -\xi_{SBR} \csc \theta_o, \quad (3.35)$$

$$Y_{SBR} = \pm \sqrt{\eta_{SBR} + a^2 \cos^2 \theta_o - \xi_{SBR}^2 \cot^2 \theta_o}. \quad (3.36)$$

In the equatorial plane $\theta = \pi/2$, X_{SBR} and Y_{SBR} reduce to

$$X_{SBR} = -\xi_{KR} + \beta \gamma_2, \quad (3.37)$$

$$Y_{SBR} = \pm \sqrt{\eta_{KR} + \beta \gamma_1}. \quad (3.38)$$

Vanishing β , we recover the Kerr situation. In Fig.(3), we plot the shadow behaviors for certain values of the involved parameters including the stringy gravity parameter β . This figure provides various shadow sizes and shapes for different values of a and β . For fixed values of the rotating parameter, we observe that the shadows of the SBR black holes increase by decreasing β . However, the geometry deformation of the SBR black holes becomes relevant with β . For large values of a and β , we find special shadow shapes analogue to the ones appearing in the case of the Kerr black hole in the presence of Gaussian plasma distributions

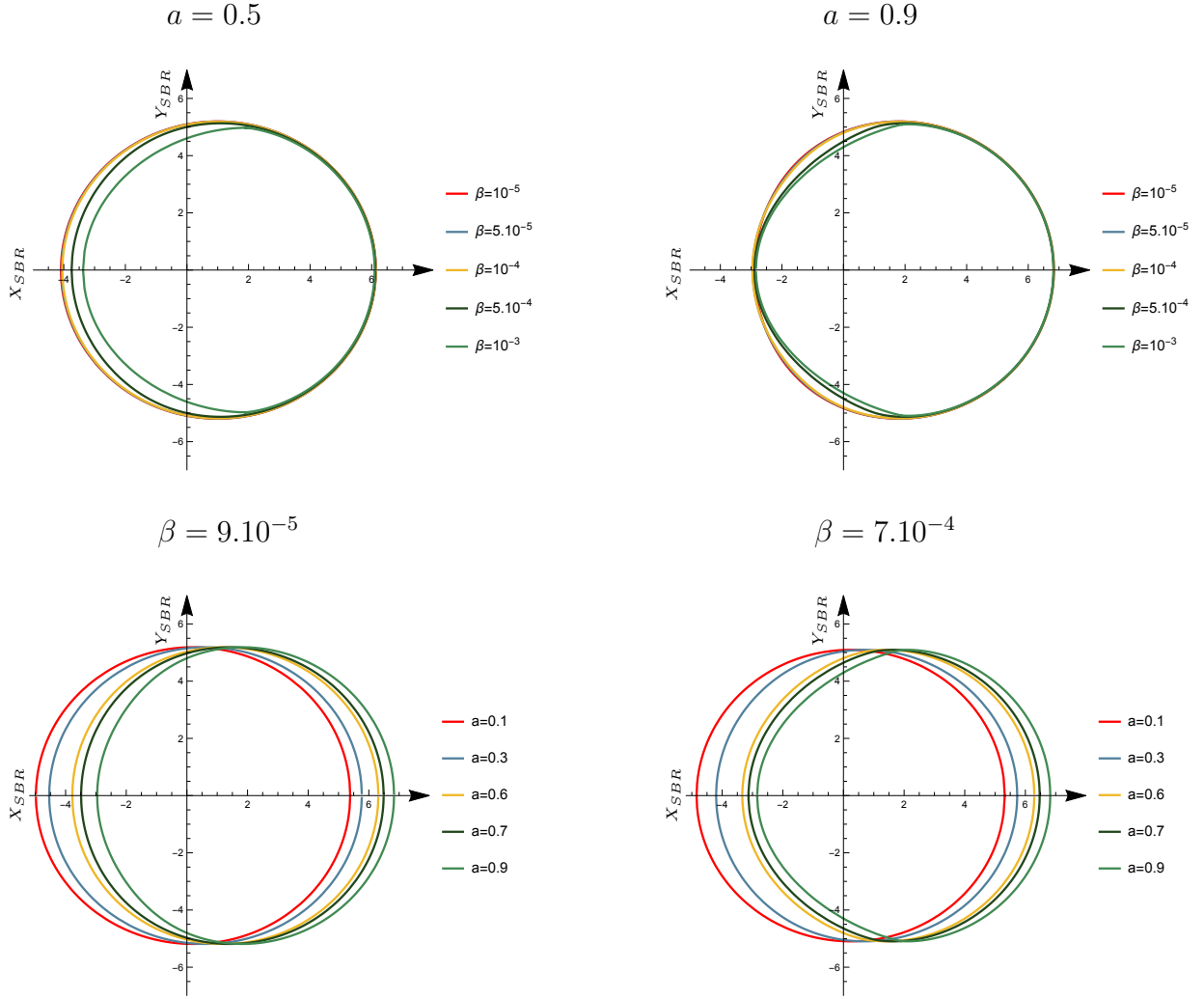


Figure 3: *Shadow shapes of SBR black holes in the equatorial plane by considering different values of a and β .*

[49, 50]. We would anticipate that the plasma and the stringy gravity parameter involve similar influences on the shadow shape of the rotating black holes. These behaviors appear for large values of a and β . To check that, we consider two values of β namely $\beta = 9.10^{-5}$ and $\beta = 7.10^{-4}$. For the first value, the shape deformations remain negligible by varying the rotating parameter. Taking $\beta = 7.10^{-4}$, however, the shape deformation becomes relevant by augmenting such a parameter.

3.2.2 Geometric deformations of the shadow

The non-trivial shadow geometries of the SBR black holes motivate one to inspect the associated deformations. The geometric deformations usually can be approached in terms of two parameters namely R_c and δ_c controlling the size and the shape, respectively. In order to examine such parameters, Fig.(4) illustrates the shadow deformations in terms of a refer-

ence circle represented by the blue color. It is recalled that R_c denotes the shadow maximal

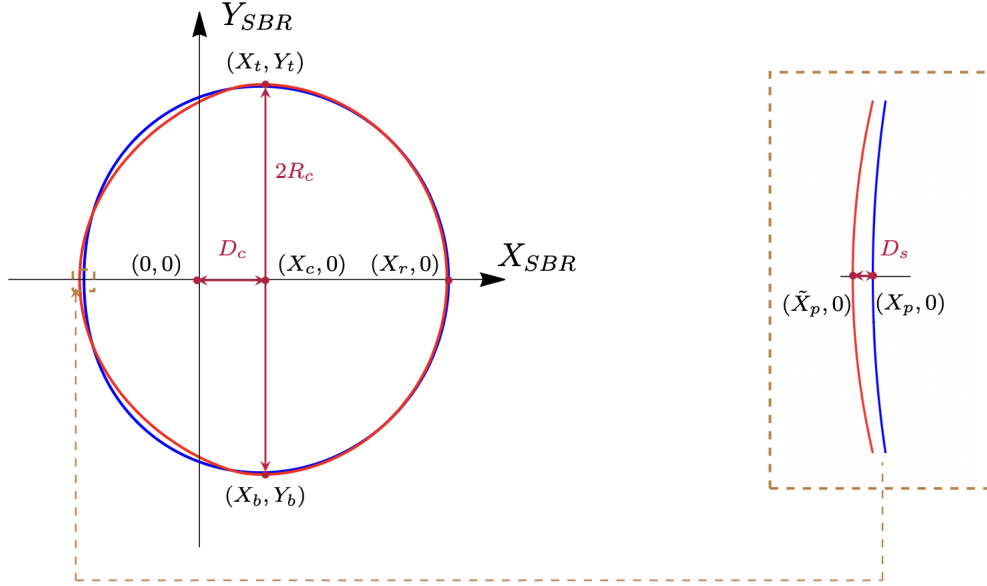


Figure 4: *Illustration of shadows size and shape parameter of SBR black hole. The reference circle is represent by the blue color and the red geometry is associated with the shadow of SBR black hole.*

radius passing through three extreme points. According to [32, 34, 35], two ones are given by the upper and the lower positions of the shadow being (X_t, Y_t) and (X_b, Y_b) , respectively. However, the remaining one is identified with either the reference circle $(X_p, 0)$ or $(\tilde{X}_p, 0)$ of the shadow geometry. In the perfect circular geometries, they coincide. The displacement D_c of the shadow from the centre can be obtained by computing

$$D_c = X_r - R_c \quad (3.39)$$

where R_c is the shadow maximal radius which could be computed from the relation

$$R_c = \frac{Y_t - Y_b}{2}. \quad (3.40)$$

In this way, the shape parameter δ_s can be expressed as follows

$$\delta_c = \frac{D_s}{R_c} = \frac{|\tilde{X}_p - X_p|}{R_c}. \quad (3.41)$$

To examine the geometric deformations, we approach R_c , D_c and δ_c by varying the rotating and the stringy gravity parameters. Fig.(5) illustrates the corresponding computations. Fixing the rotating parameter, the shadow size decreases by increasing β . However, the displacement of the shadow centre and the distortion deformation increases with the stringy gravity parameter. It has been remarked that δ_c takes higher values for a large rotating parameter. Fixing the stringy gravity parameter β , the shadow size of the SBR black holes remains almost constant even we vary a . It has been observed that the right displacement

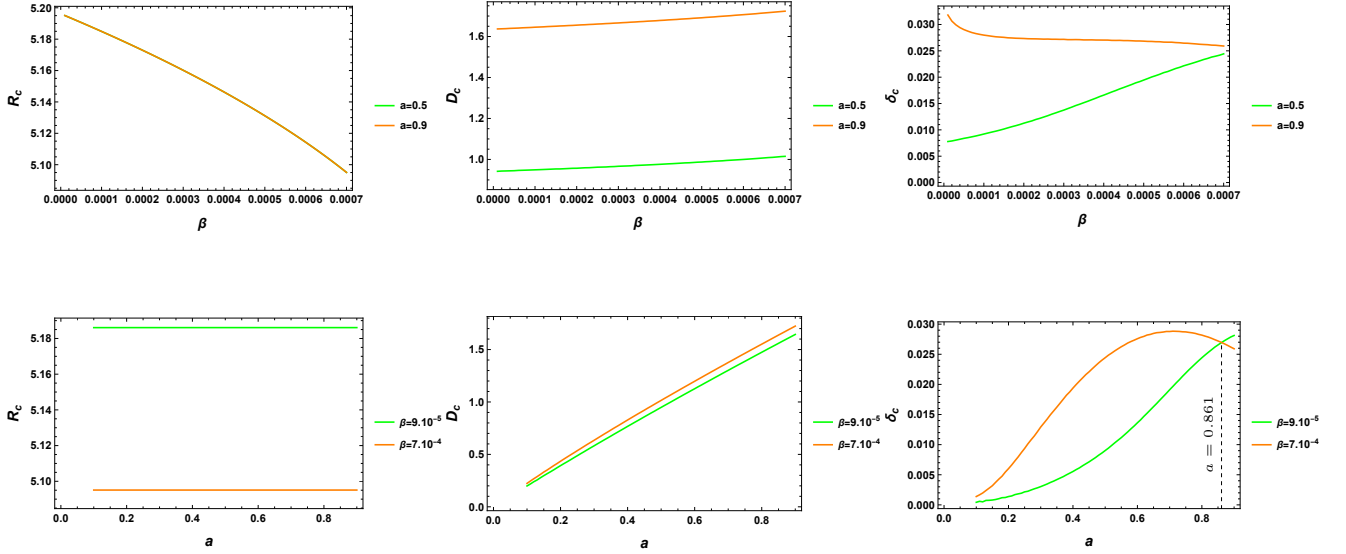


Figure 5: *Deformation observation quantities of SBR black hole as function of the rotating parameter and the string parameter.*

of the shadow increases with a via a linear behavior. In addition, we remark that the shadow shape deformation becomes relevant by increasing the rotating parameter. Taking $\beta = 7.10^{-4}$, for instance, the values of the deformation parameter takes values bigger than the case of $\beta = 9.10^{-5}$. A close examination shows that, for $a = 0.861$, a critical behavior where the curves intersect. For $\beta = 7.10^{-4}$, this intersecting point provides a changing of such a distortion behavior. This change could be explained by the existence of a pair of cusps in the shadow shape which matches with the previous shadow illustrations. For a specific range of β , we remark certain similarities between the shadow sizes of the SBR black holes and the Kerr black hole ones [46–48]. Precisely, the shape deformation of the SBR black holes could be compared with the case of the Kerr black hole in plasma backgrounds [49, 50]. This observation may deserve a concrete investigation in future works.

3.2.3 Energy emission rate

To complete the discussion of the shadow properties of the SBR black holes, we study the associated energy emission rate by considering appropriate approximations [54]. In the limit of the high energies with a far distant observer, the absorption cross-section is considered as a geometrical optical limit corresponding to the black hole shadows. In fact, this could oscillate around this geometrical limit approached in terms of the geodesic behaviors. Following [54], the energy emission rate reads as

$$\frac{d^2 E(\omega)}{d\omega dt} = \frac{2\pi^3 R_c^2}{e^{\frac{\omega}{T_h}} - 1} \omega^3 \quad (3.42)$$

where T_h and $E(\omega)$ represent the Hawking temperature and the energy of the black hole as functions of the frequency ω , respectively. R_c denotes the shadow radius. In the present

work, the Hawking temperature can be obtained via the relation

$$T_h = \frac{\Delta'(r)}{4\pi(r^2 + a^2)} \Big|_{r=r_h} \quad (3.43)$$

where r_h is the event horizon radius. This temperature is found to be

$$T_h = \frac{2(794624\pi^3\beta G^7 M^4 - 387072\pi^3\beta G^6 M^3 r - 5GM r^9 + 5r^{10})}{5r^9(a^2 + r^2)} \Big|_{r=r_h}. \quad (3.44)$$

As usually, we study the energy emission rate behaviors as a function of the stringy gravity parameter β . Fig.(6) illustrates the variation of the energy emission rate with respect to the frequency. In the left panel of the figure, we discuss the rotating parameter effect by

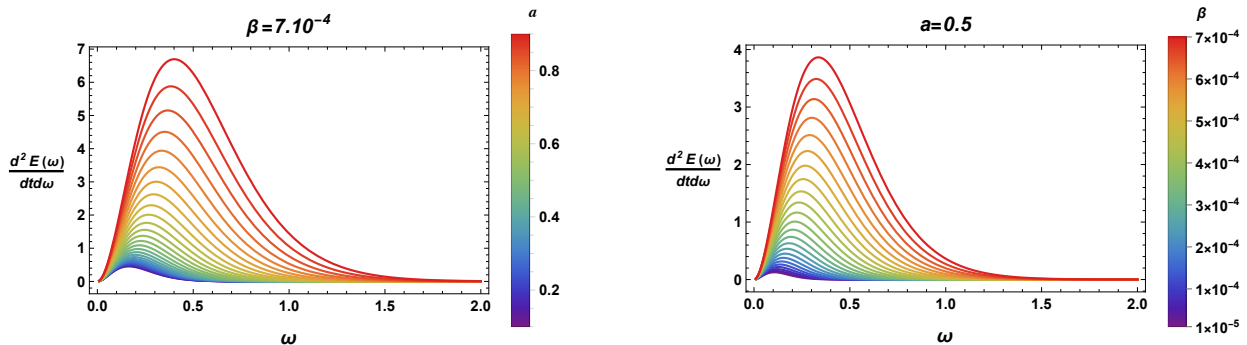


Figure 6: *Energy emission rate behaviors of SBR black hole by varying a and β parameters.*

fixing β . It follows that the energy emission rate augments with the rotating parameter. We observe that higher values of such energies correspond to large values of a . Taking $a = 0.5$, we discuss the effect of β in the right panel. Precisely, we remark that the energy emission rate increases by increasing β . A close examination shows that the evaporation scenario of the SBR black holes is fast compared to the Kerr black hole and the non-rotating ones [19, 35, 55, 56]. Moreover, we could anticipate that the energy emission rate of the SBR black holes could involve similarities with the case of the Kerr black holes in the presence of plasma [57, 58].

3.2.4 Constraints on the stringy gravity parameter via EHT observational data

In this subsection, we would like to constrain the stringy gravity parameter by means of EHT observational data. A close examination reveals that the observational data corresponding to the shadow of the supermassive black hole $M87^*$, provided by the EHT international collaborations, could be exploited to test and probe the proposed gravity models. It has been shown that such an empiric exam could impose constraints on the black hole parameters in question [35, 59–64]. In the unit of the $M87^*$ mass, we could superpose the $M87^*$ black hole

shadow behaviors given by a Kerr solution and the SBR black holes. Fixing the rotating parameter, we can confront the present gravity model with the observational fundings. In Fig.(7), we give two shadow configurations associated with two rotating parameter values. It has been observed that the rotating parameter and the $M87^*$ shadow data could fix

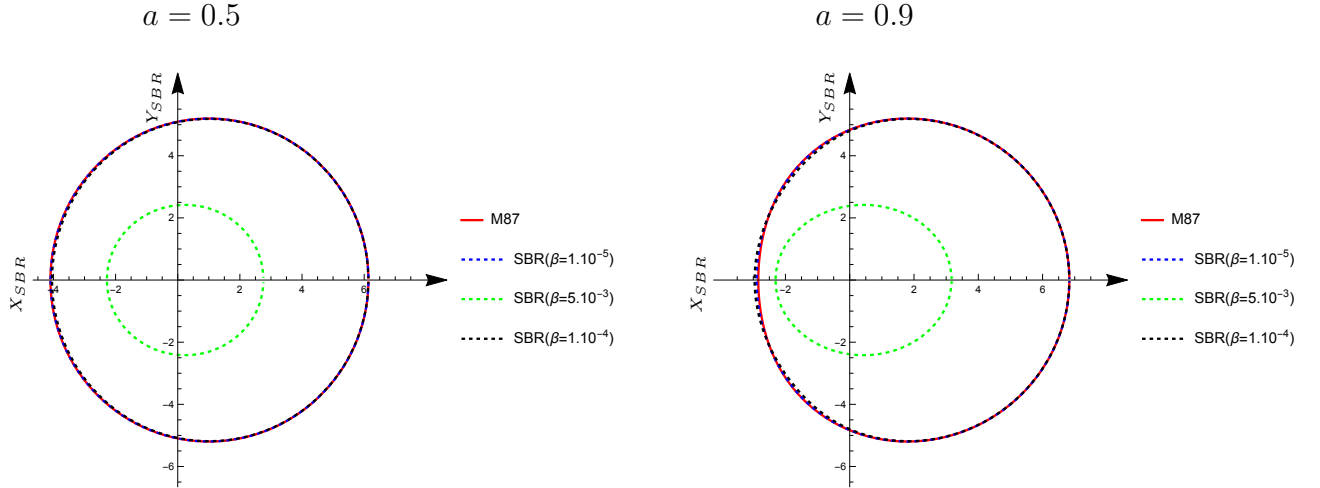


Figure 7: *SBR Black hole shadows for different values of β and a compared with $M87^*$. We take the $M87$ black hole mass $M_{BH} = 6.5 \times 10^9 M_{\odot}$ and $r_0 = 91.2 kpc$.*

the stringy gravity parameter β originated from the M-theory compactification. A close comparison between the shadow radius of the SBR and the $M87^*$ black holes conforms that the SBR shadows could coincide perfectly with the $M87^*$ ones for specific values of the stringy gravity parameter. The possible compatibilities impose the following constraint on β

$$\beta < 10^{-4}. \quad (3.45)$$

Alternative studies associated with the cosmological building models in the SBR gravity support such a constraint [46–48]. For $\beta > 10^{-4}$, however, we remark distinctions between both black hole shadows. In what follows, we consider such constraints to investigate the deflection angle of the light rays near to the proposed rotating black holes in the SBR gravity.

4 Light ray behaviors near to SBR black holes

In this section, we investigate the light ray behavior near to the SBR black holes by considering the deflection angle using the Gauss Bonnet theorem results [65]. Precisely, we would like to examine the impact of the stringy gravity parameter β on the deflection angle of the light rays by the SBR black holes. In the equatorial plane, the deflection angle can be expressed

$$\alpha = \Psi_R - \Psi_S + \phi_{SR} \quad (4.1)$$

where Ψ_R and Ψ_S are the angles between the light rays and the radial direction at the observer and the source positions, respectively. It is denoted that ϕ_{SR} is the longitude separation angle [66]. To obtain such an optical quantity, we could adopt the algorithm developed in [67]. Taking the following line element

$$ds^2 = -A(r, \theta)dt^2 + B(r, \theta)dr^2 + C(r, \theta)d\theta^2 + D(r, \theta)d\phi^2 - 2H(r, \theta)dtd\phi, \quad (4.2)$$

we can compute the above angular quantities [67]. The ψ terms can be extracted from the following equation

$$\sin \Psi = \frac{H(r) + A(r)b}{\sqrt{A(r)D(r) + H^2(r)}} \quad (4.3)$$

where b is identified with the impact parameter $\frac{L}{E}$. Placing the observer (R) and the source (S) at a finite distance and making the change of variable $u = \frac{1}{r}$, the separation angle takes the form

$$\phi_{RS} = \int_S^R d\phi = \int_{u_S}^{u_0} \frac{1}{\sqrt{F(u)}} du + \int_{u_0}^{u_R} \frac{1}{\sqrt{F(u)}} du \quad (4.4)$$

u_S and u_R denote the inverse of the source and the observer distance from the black hole, respectively. u_0 is the inverse of the closest approach r_0 . The $F(u)$ function is expressed as follows

$$F(u) = \left(\frac{1}{u^2} \frac{du}{d\phi} \right)^2. \quad (4.5)$$

The computations lead to

$$F(u) = \frac{u^4 (A(u) D(u) + H(u)^2) (b^2 (-A(u)) - 2bH(u) + D(u))}{B(u) (bA(u) + H(u))^2}. \quad (4.6)$$

Having given the essential on the deflection angle terms, we move to compute its explicit expressions for both cases: non-rotating and rotating solutions.

4.1 Deflection angle of non-rotating solutions

To start the deflection angle computations, we consider the non-rotating solutions of the SBR black holes. The calculations give

$$\begin{aligned}
\phi_{RS} &= (\pi - \arcsin(bu_R) - \arcsin(bu_S)) + \left(\frac{2 - b^2u_R^2}{\sqrt{1 - b^2u_R^2}} + \frac{2 - b^2u_S^2}{\sqrt{1 - b^2u_S^2}} \right) \frac{GM}{b} \\
&+ (\pi - \arcsin(bu_R) - \arcsin(bu_S)) \frac{15G^2M^2}{4b^2} \\
&+ \left(\frac{u_R(3b^4u_R^4 - 20b^2u_R^2 + 15)}{(1 - b^2u_R^2)^{3/2}} + \frac{u_S(3b^4u_S^4 - 20b^2u_S^2 + 15)}{(1 - b^2u_S^2)^{3/2}} \right) \frac{G^2M^2}{4b^2} \\
&+ \left(\frac{-5b^8u_R^8 - 40b^6u_R^6 + 240b^4u_R^4 - 320b^2u_R^2 + 128}{(1 - b^2u_R^2)^{5/2}} \right. \\
&+ \left. \frac{-5b^8u_S^8 - 40b^6u_S^6 + 240b^4u_S^4 - 320b^2u_S^2 + 128}{(1 - b^2u_S^2)^{5/2}} \right) \frac{G^3M^3}{6b^3} \\
&+ \left(\frac{7b^{10}u_R^{10} + 10b^8u_R^8 + 16b^6u_R^6 + 32b^4u_R^4 + 128b^2u_R^2 - 256}{\sqrt{1 - b^2u_R^2}} \right. \\
&+ \left. \frac{7b^{10}u_S^{10} + 10b^8u_S^8 + 16b^6u_S^6 + 32b^4u_S^4 + 128b^2u_S^2 - 256}{\sqrt{1 - b^2u_S^2}} \right) \frac{6144\pi^3\beta G^6M^3}{35b^9}. \tag{4.7}
\end{aligned}$$

For the Ψ expressions, we find

$$\begin{aligned}
\Psi_R - \Psi_S &= (\arcsin(bu_R) + \arcsin(bu_S) - \pi) - \left(\frac{u_R^2}{\sqrt{1 - b^2u_R^2}} + \frac{u_S^2}{\sqrt{1 - b^2u_S^2}} \right) bGM \\
&+ \left(\frac{u_R^3(2b^2u_R^2 - 1)}{(1 - b^2u_R^2)^{3/2}} + \frac{u_S^3(2b^2u_S^2 - 1)}{(1 - b^2u_S^2)^{3/2}} \right) \frac{bG^2M^2}{2} + \left(\frac{u_R^4(-8b^4u_R^4 + 8b^2u_R^2 - 3)}{(1 - b^2u_R^2)^{5/2}} \right. \\
&+ \left. \frac{u_S^4(-8b^4u_S^4 + 8b^2u_S^2 - 3)}{(1 - b^2u_S^2)^{5/2}} \right) \frac{bG^3M^3}{6} + \left(\frac{u_R^{10}}{\sqrt{1 - b^2u_R^2}} + \frac{u_S^{10}}{\sqrt{1 - b^2u_S^2}} \right) \frac{55296\pi^3b\beta G^6M^3}{5}. \tag{4.8}
\end{aligned}$$

Combining the obtained expressions, we get

$$\begin{aligned}
\alpha &= \left(\sqrt{1 - b^2u_R^2} + \sqrt{1 - b^2u_S^2} \right) \frac{2GM}{b} + (\pi - \arcsin(bu_R) - \arcsin(bu_S)) \frac{15G^2M^2}{4b^2} \\
&+ \left(\frac{15bu_R - 7b^3u_R^3}{\sqrt{1 - b^2u_R^2}} + \frac{15bu_S - 7b^3u_S^3}{\sqrt{1 - b^2u_S^2}} \right) \frac{G^2M^2}{4b^2} \\
&+ \left(\frac{13b^6u_R^6 + 45b^4u_R^4 - 192b^2u_R^2 + 128}{(1 - b^2u_R^2)^{3/2}} + \frac{13b^6u_S^6 + 45b^4u_S^4 - 192b^2u_S^2 + 128}{(1 - b^2u_S^2)^{3/2}} \right) \frac{G^3M^3}{6b^3} \\
&+ \left(\frac{35b^{10}u_R^{10} + 5b^8u_R^8 + 8b^6u_R^6 + 16b^4u_R^4 + 64b^2u_R^2 - 128}{\sqrt{1 - b^2u_R^2}} \right. \\
&+ \left. \frac{35b^{10}u_S^{10} + 5b^8u_S^8 + 8b^6u_S^6 + 16b^4u_S^4 + 64b^2u_S^2 - 128}{\sqrt{1 - b^2u_S^2}} \right) \frac{12288\pi^3\beta G^6M^3}{35b^9}. \tag{4.9}
\end{aligned}$$

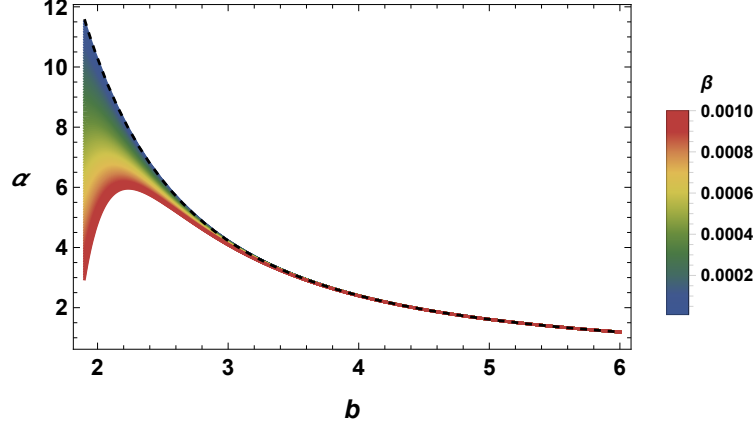


Figure 8: Variation of deflection angle of SBR black hole in terms of the impact parameter for large range of the string parameter. Dashed black curve: variation of deflection angle of Schwarzschild black hole.

Sending u_R and u_S to zero, we can obtain an approximated expression of the deflection angle of the light rays near to the non-rotating SBR black holes. Indeed, it is given by

$$\alpha \simeq \frac{4GM}{b} + \frac{15\pi G^2 M^2}{4b^2} + \frac{128G^3 M^3}{3b^3} - \frac{3145728\pi^3 \beta G^6 M^3}{35b^9}. \quad (4.10)$$

The deflection angle depends on M , b and the stringy gravity parameter β . The previous shadow investigation has revealed that certain constraints on β should be imposed. Taking into account such conditions, we present this deflection angle of light rays as a function of the impact parameter by varying the stringy gravity parameter β . Fig.(8) illustrates this variation for different values of β . For small values of b , we remark a considerable effect of β on the deflection angle. Precisely, it decreases by increasing β . For large values of b , we do not observe a relevant distinction due to coinciding curves of the deflection angle of the light rays. In this region of the moduli space, the deflection angle decreases slightly.

4.2 Deflection angle of rotating SBR black holes

Here, we investigate the impact of the stringy gravity parameter β on the deflection angle of the light rays by rotating black holes in the SBR gravity. Using similar calculations, we can obtain the following separation angle for the slowly rotating black holes. Indeed, we find

$$\begin{aligned} \phi_{RS_a} = & \phi_{RS} - \left(\frac{1}{\sqrt{1-b^2u_R^2}} + \frac{1}{\sqrt{1-b^2u_S^2}} \right) \frac{2GMa}{b^2} + (\arcsin(bu_R) + \arcsin(bu_S) - \pi) \frac{10G^2M^2a}{b^3} \\ & + \left(\frac{bu_R(6b^2u_R^2-5)}{(1-b^2u_R^2)^{3/2}} + \frac{bu_S(6b^2u_S^2-5)}{(1-b^2u_S^2)^{3/2}} \right) \frac{2G^2M^2a}{b^3} + \left(\frac{35b^6u_R^6 - 182b^4u_R^4 + 240b^2u_R^2 - 96}{(1-b^2u_R^2)^{5/2}} \right. \\ & + \left. \frac{35b^6u_S^6 - 182b^4u_S^4 + 240b^2u_S^2 - 96}{(1-b^2u_S^2)^{5/2}} \right) \frac{G^3M^3a}{b^4} - \left(\frac{5b^8u_R^8 + 8b^6u_R^6 + 16b^4u_R^4 + 64b^2u_R^2 - 128}{\sqrt{1-b^2u_R^2}} \right. \\ & \left. + \frac{5b^8u_S^8 + 8b^6u_S^6 + 16b^4u_S^4 + 64b^2u_S^2 - 128}{\sqrt{1-b^2u_S^2}} \right) \frac{110592\pi^3\beta G^6M^3a}{175b^{10}}. \end{aligned} \quad (4.11)$$

The remaining deflection angle equation can be expressed as follows

$$\begin{aligned}
\Psi_{RS_a} &= \Psi_{RS} + \left(\frac{u_R^2}{\sqrt{1-b^2u_R^2}} + \frac{u_S^2}{\sqrt{1-b^2u_S^2}} \right) 2GMa - \left(\frac{u_R^3(2b^2u_R^2-1)}{(1-b^2u_R^2)^{3/2}} + \frac{u_S^3(2b^2u_S^2-1)}{(1-b^2u_S^2)^{3/2}} \right) 2G^2M^2a \\
&+ \left(\frac{u_R^4(8b^4u_R^4-8b^2u_R^2+3)}{(1-b^2u_R^2)^{5/2}} + \frac{u_S^4(8b^4u_S^4-8b^2u_S^2+3)}{(1-b^2u_S^2)^{5/2}} \right) G^3M^3a \\
&- \left(\frac{u_R^{10}}{\sqrt{1-b^2u_R^2}} + \frac{u_S^{10}}{\sqrt{1-b^2u_S^2}} \right) \frac{110592}{5} \pi^3 \beta G^6 M^3 a
\end{aligned} \tag{4.12}$$

where the notation $\Psi_{RS_a} = \Psi_{R_a} - \Psi_{S_a}$ has been used. Using the above equations, the expression of the deflection angle of light rays of the rotating SBR black holes is found to be

$$\begin{aligned}
\alpha_{RS_a} &= \alpha_{RS} - \frac{2aGM}{b^2} \left(\sqrt{1-b^2u_R^2} + \sqrt{1-b^2u_S^2} \right) + \frac{2aG^2M^2}{b^3} \left(\frac{2b^3u_R^3-5bu_R}{\sqrt{1-b^2u_R^2}} + \frac{2b^3u_S^3-5bu_S}{\sqrt{1-b^2u_S^2}} \right) \\
&+ \frac{10aG^2M^2}{b^3} (\arcsin(bu_R) + \arcsin(bu_S) - \pi) - \frac{aG^3M^3}{b^4} \left(\frac{8b^6u_R^6+35b^4u_R^4-144b^2u_R^2+96}{(1-b^2u_R^2)^{3/2}} \right. \\
&+ \left. \frac{8b^6u_S^6+35b^4u_S^4-144b^2u_S^2+96}{(1-b^2u_S^2)^{3/2}} \right) \\
&+ \frac{110592\pi^3a\beta G^6M^3}{175b^{10}} \left(\sqrt{1-b^2u_R^2} (35b^8u_R^8+40b^6u_R^6+48b^4u_R^4+64b^2u_R^2+128) \right. \\
&+ \left. \sqrt{1-b^2u_S^2} (35b^8u_S^8+40b^6u_S^6+48b^4u_S^4+64b^2u_S^2+128) \right).
\end{aligned} \tag{4.13}$$

Taking appropriate limits, we can get such the expression of the deflection angle of light rays in the SBR gravity. Indeed, it takes the form

$$\begin{aligned}
\alpha_a &\simeq \frac{4GM}{b} + \frac{15\pi G^2M^2}{4b^2} + \frac{128G^3M^3}{3b^3} - \frac{3145728\pi^3\beta G^6M^3}{35b^9} - \frac{4aGM}{b^2} - \frac{10\pi aG^2M^2}{b^3} - \frac{192aG^3M^3}{b^4} \\
&+ \frac{28311552\pi^3a\beta G^6M^3}{175b^{10}}.
\end{aligned} \tag{4.14}$$

Considering $a = 0$, we obtain the deflection angle of the non-rotating solutions obtained in the previous section. For $\beta = 0$, we recover the case of the Kerr solution. By fixing the rotating parameter, we illustrate in Fig.(9) the deflection angle as a function of b by varying the stringy gravity parameter β in the range obtained by the above computations associated with EHT requirements.

For small values of the impact parameter and the rotating parameter, we can observe a relevant effect of the stringy gravity parameter which decreases the deflection angle. It follows from the figure that the deflection angle decreases with the rotating parameter. For large values of the rotating parameter the β -curves are not distinguishable, with respect to the Kerr ones. This could show that, for large rotating parameter values, the effect of β becomes irrelevant. In Fig.(10), we present the variation of the deflection angle in terms of the impact parameter by varying the rotating parameter and fixing the stringy gravity parameter. Contrary to the shadow behavior, the two fixed values of β provide similar

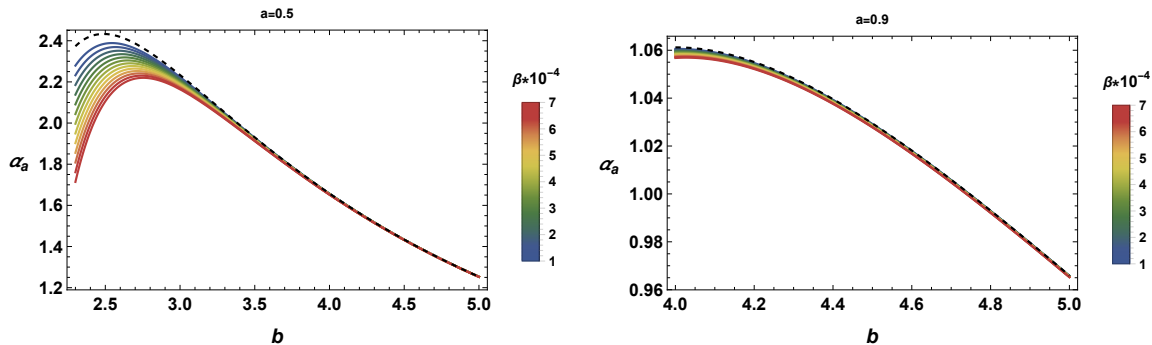


Figure 9: Deflection angle of the light rays near to the rotating SBR black holes as a function of the impact parameter by varying β and fixing a .

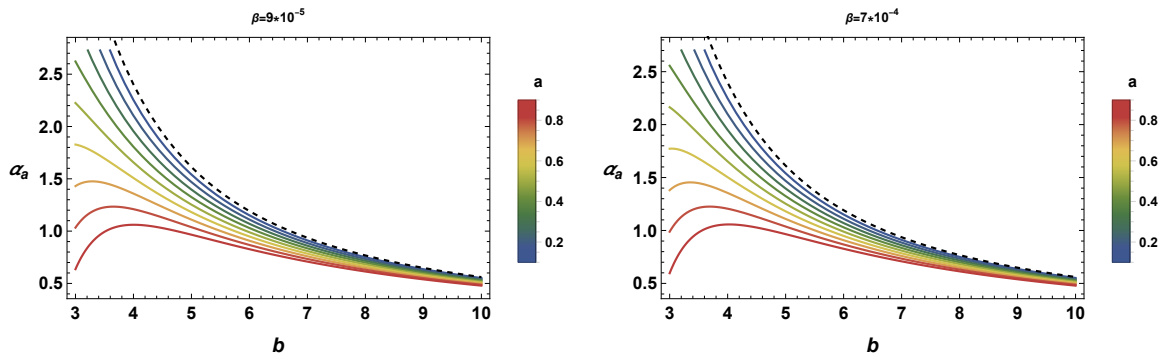


Figure 10: Deflection angle of light rays near rotating SBR black holes as a function of the impact parameter by varying a and fixing β .

behaviors. Moreover, the decreasing behavior of the deflection angle depends on both the rotating parameter and the stringy gravity one. The associated critical impact parameter is shifted by increasing such parameters.

5 Conclusion

Motivated by M-theory compactifications, we have studied optical properties of the black holes in the SBR gravity. Precisely, we have discussed the shadows and the deflection angle of the light rays by non-rotating and rotating black holes in four dimensions. In the first part of this work, we have investigated the shadows of the Schwarzschild-type solutions. As expected, we have obtained perfect circular shadows where the size decreases with the stringy gravity parameter β . The latter has been constrained by $\beta < 8.10^{-2}$ derived from the shadow existence. Indeed, the radius of the horizon is small than the shadow. For $\beta > 8.10^{-2}$, however, the shadow does not exist. This constraint on β matches perfectly with certain

findings associated with the cosmological building models in the SRB gravity [47]. In such a range of the stringy gravity parameter, we have combined the Newman-Janis algorithm and the Hamilton-Jacobi mechanism to investigate the shadow behaviors of the rotating solutions in terms of one-dimensional real closed curves. More precisely, we have provided various sizes and shapes depending on the rotating and the stringy gravity parameters a and β , respectively. To examine the shadow geometric deformations, we have exploited the astronomical observables and the energy emission rate. As results, we have shown that the rotating parameter a and the stringy gravity parameter β could control the shadow aspect. For specific values of a and β , we have observed a pair of cusps in the shadow geometry of the SBR black holes. It has been remarked that such a pair of cusps has appeared in the Kerr black hole solution in plasma distribution backgrounds [49, 50]. We anticipate that the plasma and the stringy gravity parameter could have a quite similar effect on the shadow shapes. As mentioned before, this could deserve more understandings. Using EHT observational data, we have provided constraints on β which could play a relevant role in M-theory compactifications being in a good agreement with results obtained from recent cosmological investigations. Taking into account these constraints, we have elaborated a concise study on the light ray behaviors near to the SBR black holes in the SBR gravity by computing the deflection angle in terms of a and β . In particular, we have presented a graphical analysis of such a deflection angle of the light rays. We have observed that, for large values of the rotating parameter, the stringy gravity parameter does not affect the deflection angle of the light rays near to the SBR black holes.

This work comes up with open questions. A natural question concerns the link with M-theory compactifications on non-trivial geometries including the G2-manifolds. It could be possible to use the black hole physics to control the gravity parameters from observational data associated either with $M87^*$ or Sgr A* [68, 69]. In this way, the rotating black holes can play a primordial role in testing gravity models via its moduli space. Moreover, the SBR gravity has received a special interest in connections with inflation models [70]. It should be interesting to implement the coupling inflation scenario in such a gravity. It could be possible to address all these issues in future works.

Acknowledgements

The authors would like to thank N. Askour, H. El Moumni, S-E. Ennadifi, M. Lamaaoune M. Oualaid, and Y. Sekhmani for discussions and recent collaborations on related topics.

References

- [1] B. Abbott and al., *Observation of Gravitational Waves from a Binary Black Hole Merger*, Phys. Rev. Lett. **116** (6) (2016) 061102, [arXiv:1602.03837](https://arxiv.org/abs/1602.03837).

- [2] K. Akiyama and al., *First M87 Event Horizon Telescope Results. IV. Imaging the Central Supermassive Black Hole*, *Astrophys. J.* **L4** (1) (2019) 875, [arXiv:1906.11241](#).
- [3] K. Akiyama and al., *First M87 Event Horizon Telescope Results. V. Imaging the Central Supermassive Black Hole*, *Astrophys. J.* **L5** (1) (2019) 875.
- [4] K. Akiyama and al., *First M87 Event Horizon Telescope Results. VI. Imaging the Central Supermassive Black Hole*, *Astrophys. J.* **L6** (1) (2019) 875.
- [5] S.W. Hawking, H.S. Reall, *Charged and rotating AdS black holes and their CFT duals*, *Phys.Rev.D* **61** (2000) 024014, [arXiv:hep-th/9908109](#).
- [6] A. Chamblin, R. Emparan, C. V. Johnson, R. C. Myers, *Charged AdS Black Holes and Catastrophic Holography*, *Phys.Rev.D* **60** (1999) 064018, [arXiv:hep-th/9902170](#).
- [7] A. Rajagopal, D. Kubiznak, R. B. Mann, *Van der Waals black hole*, *Phys. Lett.* **B737** (2014) 277, [arXiv:1408.1105](#).
- [8] D. Kubiznak, R. B. Mann, Mae Teo, *Black hole chemistry: thermodynamics with Lambda*, *Class. Quant. Grav.* **34** (2017) 063001, [arXiv:1608.06147](#).
- [9] S. W. Hawking, D. N. Page, *Thermodynamics of black holes in anti-de Sitter space*, *Communications in Mathematical Physics* **87**(4) (1983) 577.
- [10] G.W. Gibbons, M.J. Perry, C.N. Pope, *The First Law of Thermodynamics for Kerr-Anti-de Sitter Black Holes*, *Class. Quant. Grav.* **22** (2005)1503.
- [11] A. Belhaj, M. Chabab, H. El Moumni and M. B. Sedra, *On thermodynamics of AdS black holes in arbitrary dimensions*, *Chin. Phys. Lett.* **29** (2012) 100401.
- [12] F. Barzi, H. El Moumni, *On Rényi universality formula of charged flat black holes from Hawking-Page phase transition*, *Phys. Lett. B*, **833**(2022)137378.
- [13] A. Belhaj, A. El Balali, W. El Hadri, and E. Torrente-Lujan, *On universal constants of AdS black holes from Hawking-Page phase transition*, *Phys. Lett. B.* **811**(2020)135871.
- [14] R. Banerjee, S. Ghosh and D. Roychowdhury, *New type of phase transition in Reissner Nordstrm AdS black hole and its thermodynamic geometry*, *Phys. Lett.B* **696** (2011) 156.
- [15] Y. Liu, D. C. Zou, B. Wang, *Signature of the Van der Waals like small-large charged AdS black hole phase transition in quasi normal modes*, *JHEP* **09** (2014) 179, [arXiv:1405.2644](#).
- [16] A. Belhaj, M. Chabab, H. El Moumni, K. Masmarr, M. B. Sedra, *On thermodynamics of AdS black holes in M-theory*, *Eur. Phys. J. C* **76**(2) (2016) 73.

- [17] A. Belhaj, H. Belmahi, M. Benali, W. El Hadri, H. El Moumni, E. Torrente-Lujan, *Shadows of 5D Black Holes from string theory*, Phys. Lett. B **812** (2021) 136025, [arXiv:2008.13478](#).
- [18] A. Belhaj, H. Belmahi, M. Benali, *Superentropic AdS black hole shadows*, Phys. Lett. B **821** (2021) 136619, [arXiv:2110.06771](#).
- [19] A. Belhaj, M. Benali, A. El Balali, H. El Moumni and S-E. Ennadifi, *Deflection angle and shadow behaviors of quintessential black holes in arbitrary dimensions*, Class. Quantum Grav. **37** (2020) 215004, [arXiv:2006.01078](#).
- [20] W. Javed, J. Abbas, and A. Övgün, *Deflection angle of photon from magnetized black hole and effect of nonlinear electrodynamics*, Eur. Phys. J. C **79** (2019) 694, [arXiv:1908.09632](#).
- [21] A. Belhaj, H. Belmahi, M. Benali, *Deflection Light Behaviors by AdS Black Holes*, Gen.Rel.Grav. **79** 54 (2022) 4, [arXiv:2112.06215](#).
- [22] A. Belhaj, H. Belmahi, M. Benali, H. El Moumni, *Light Deflection by Rotating Regular Black Holes with a Cosmological Constant*, [arXiv:2204.10150](#).
- [23] W. Javed, J. Abbas, and A. Övgün, *Deflection angle of photon from magnetized black hole and effect of nonlinear electrodynamics*, Eur. Phys. J. C **79** (2019) 694, [arXiv:1908.09632](#).
- [24] A. Belhaj, H. Belmahi, M. Benali and H. El Moumni, *Light deflection angle by super-entropic black holes*, Int. J. Mod. Phys. D **31** (2022) 2250054, [arXiv:2203.11143](#).
- [25] A. Belhaj, H. Belmahi, M. Benali and A. Segui, *Thermodynamics of AdS black holes from deflection angle formalism*, Phys. Lett. B **817** (2021) 136313.
- [26] C. A. R. Herdeiro, A. M. Pombo, E. Radu, P. V. P. Cunha and N. Sanchis-Gual, *The imitation game: Proca stars that can mimic the Schwarzschild shadow*, JCAP **04** (2021) 051, [arXiv:2102.01703](#).
- [27] C. A. R. Herdeiro, A. M. Pombo, E. Radu, P. V. P. Cunha and N. Sanchis-Gual, *The imitation game: Proca stars that can mimic the Schwarzschild shadow*, JCAP **04** (2021) 051, [arXiv:2102.01703](#).
- [28] S. W. Wei, Y. C. Zou, Y. X. Liu, R. B. Mann, *Curvature radius and Kerr black hole shadow*, JCAP **08** (2019) 030, [arXiv:1904.07710](#).
- [29] J. R. Farah, D. W. Pesce, M. D. Johnson, L. L. Blackburn, *On the approximation of the black hole shadow with a simple polar curve*, Astrophys. J. **900** (2020) 77, [arXiv:2007.06732](#).

- [30] S. V. M. C. B. Xavier, P. V. P. Cunha, L. C. B. Crispino, C. A. R. Herdeiro, *Shadows of charged rotating black holes: Kerr–Newman versus Kerr–Sen*, Int. J. Mod. Phys. D **29** (2020) 2041005, arXiv:2003.14349.
- [31] S. U. Khan, J. Ren, *Shadow cast by a rotating charged black hole in quintessential dark energy*, Phys. Dark Univ. **30** (2020) 100644, arXiv:2006.11289.
- [32] X. Hou, Z. Xu, J. Wang, *Rotating black hole shadow in perfect fluid dark matter*, JCAP **12** (2018) 040.
- [33] A. Belhaj, M. Benali and Y. Hassouni, *Superentropic black hole shadows in arbitrary dimensions*, Eur. Phys. J. C **82** (2022) 619, arXiv:2203.06774.
- [34] A. Belhaj, H. Belmahi and M. Benali, *Superentropic AdS black hole shadows*, Phys. Lett. B **821** (2021) 136619, arXiv:2110.06771.
- [35] A. Belhaj, M. Benali, A. El Balali, W. El Hadri, H. El Moumni, E. Torrente-Lujan, *Black hole shadows in M-theory scenarios*, Int. J. Mod. Phys. D **30** (2021) 2150026, arXiv:2008.09908.
- [36] A. Belhaj, A. El Balali, W. El Hadri, Y. Hassouni, E. Torrente-Lujan, *Phase transition and shadow behaviors of quintessential black holes in M-theory/superstring inspired models*, Int. J. Mod. Phys. A **36** (2021) 2150057, arXiv:2004.10647.
- [37] N. Askour, A. Belhaj, H. Belmahi, M. Benali, H. El Moumni, Y. Sekhmani, *Light Behaviors around Black Holes in M-theory*, arXiv:2301.08321.
- [38] J. T. Wheeler, *Symmetric solutions to the Gauss-Bonnet extended Einstein equations*, Nucl. Phys. B **268** (1986) 737.
- [39] S. G. Ghosh, R. Kumar, *Generating black holes in 4D Einstein-Gauss-Bonnet gravity*, Class.Quant.Grav. **37** (2020) 245008, arXiv:2003.12291.
- [40] S. G. Ghosh, S. D. Maharaj, *Radiating black holes in the novel 4D Einstein-Gauss-Bonnet gravity*, Phys. Dark Univ. **30** (2020) 100687, arXiv:2003.09841.
- [41] S. G. Ghosh, D. V. Singh, R. Kumar, S. D. Maharaj, *Phase transition of AdS black holes in 4D EGB gravity coupled to nonlinear electrodynamics*, Annals of Physics **424**(2021)168347, arXiv:2006.00594.
- [42] D. V. Singh, B. K. Singh, S. Upadhyay, *4D AdS Einstein–Gauss–Bonnet black hole with Yang–Mills field and its thermodynamics*, Annals of Physics **434**(2021) 168642.
- [43] A. Belhaj, Y. Sekhmani, *Optical and thermodynamic behaviors of Ayón–Beato–García black holes for 4D Einstein Gauss–Bonnet gravity*, Annals of Physics **441**(2022)168863.

- [44] A. Belhaj, Y. Sekhmani, *Thermodynamics of Ayon-Beato–Garcia–AdS black holes in 4D Einstein–Gauss–Bonnet gravity*, Eur. Phys. J. Plus **137**(2022)278.
- [45] S. Vagnozzi, R. Roy, Yu-Dai Tsai, L. Visinelli, M. Afrin, A. Allahyari, P. Bambhaniya, D. Dey, S. G. Ghosh, P. S. Joshi, K. Jusufi, M. Khodadi, R. K. Walia, A. Övgün, C. Bambi, *Horizon-scale tests of gravity theories and fundamental physics from the Event Horizon Telescope image of Sagittarius A**, arXiv:2205.07787.
- [46] S. V. Ketov, *Starobinsky-Bel-Robinson gravity*, Universe **8** (2022) 351, arXiv:2205.13172.
- [47] S. V. Ketov, E. O. Pozdeeva, S. Yu. Vernov, *On the superstring-inspired quantum correction to the Starobinsky model of inflation*, JCAP **12** (2022) 032, arXiv:2211.01546.
- [48] R. C. Delgado, S. V. Ketov, *Schwarzschild-type black holes in Starobinsky-Bel-Robinson gravity*, Phys. Lett. B **838** (2023) 137690, arXiv:2209.01574.
- [49] Z. Zhang, H. Yan, M. Guo and B. Chen, *Shadows of Kerr black holes with a Gaussian-distributed plasma in the polar direction*, Phys. Rev. D **107** (2023) 024027, arXiv:2206.04430.
- [50] Y. Huang, Y. P. Dong and D. J. Liu, *Revisiting the shadow of a black hole in the presence of a plasma*, Int. J. Mod. Phys. D **27** (2018) 1850114, arXiv:1807.06268.
- [51] E. Witten, *Solutions of four-dimensional field theories via M-theory*, Nucl. Phys. B **500** (1997) 42.
- [52] S. P. Drake P. Szekeres, *An explanation of the Newman-Janis Algorithm*, Gen.Rel.Grav. **32** (2000) 445, arXiv:gr-qc/9807001.
- [53] Harold Erbin, *Janis-Newman algorithm: generating rotating and NUT charged black holes*, Universe **3** (2017) 19, arXiv:1701.00037.
- [54] S. W. Wei and Y. X. Liu, *Observing the shadow of Einstein-Maxwell-Dilaton-Axion black hole*, JCAP **11** (2013) 063, arXiv:1311.4251.
- [55] A. Belhaj, M. Benali, H. El Moumni, M. A. Essebani, M. B. Sedra and Y. Sekhmani, *Thermodynamic and optical behaviors of quintessential Hayward-AdS black holes*, Int. J. Geom. Meth. Mod. Phys. **19** (2022) 2250096, arXiv:2202.06290.
- [56] A. Belhaj, M. Benali, A. E. Balali, W. E. Hadri and H. El Moumni, *Cosmological constant effect on charged and rotating black hole shadows*, Int. J. Geom. Meth. Mod. Phys. **18** (2021) 2150188, arXiv:2007.09058.
- [57] F. Atamurotov and B. Ahmedov, *Optical properties of black hole in the presence of plasma: shadow*, Phys. Rev. D **92** (2015) 084005, arXiv:1507.08131.

- [58] G. Z. Babar, A. Z. Babar and F. Atamurotov, *Optical properties of Kerr–Newman spacetime in the presence of plasma*, Eur. Phys. J. C **80** (2020) 761, [arXiv:2008.05845](#).
- [59] C. Bambi, K. Freese, S. Vagnozzi, L. Visinelli, *Testing the rotational nature of the supermassive object M87* from the circularity and size of its first image*, Phys. Rev. D **100** (2019) 044057, [arXiv:1904.12983](#).
- [60] S. Vagnozzi, L. Visinelli, *Hunting for extra dimensions in the shadow of M87**, Phys. Rev. D **100** (2019) 024020, [arXiv:1905.12421](#).
- [61] A. Allahyari, M. Khodadi, S. Vagnozzi, D. F. Mota, *Magnetically charged black holes from non-linear electrodynamics and the Event Horizon Telescope*, JCAP **2002** (2020) 003, [arXiv:1912.08231](#)
- [62] M. Khodadi, A. Allahyari, S. Vagnozzi, D. F. Mota, *Black holes with scalar hair in light of the Event Horizon Telescope*, JCAP **2009** (2020) 026, [arXiv:2005.05992](#)
- [63] R. Roy, S. Vagnozzi, L. Visinelli, *Superradiance evolution of black hole shadows revisited*, Phys. Rev. D **05** (2022) 083002, [arXiv:2112.06932](#).
- [64] S. Vagnozzi, C. Bambi, L. Visinelli, *Concerns regarding the use of black hole shadows as standard rulers*, Class. Quant. Grav. **37** (2020) 087001, [arXiv:2001.02986](#).
- [65] T. Ono, A. Ishihara, H. Asada, *Gravitomagnetic bending angle of light with finite-distance corrections in stationary axisymmetric spacetimes*, Phys. Rev. D **96** (2017) 104037, [arXiv:1704.05615](#).
- [66] R. C. Pantig and E. T. Rodulfo, *Weak deflection angle of a dirty black hole*, Chin. J. Phys. **66** (2020) 691, [arXiv:2003.00764](#).
- [67] A. Ishihara, Y. Suzuki, T. Ono, T. Kitamura, H. Asada, *Gravitational bending angle of light for finite distance and the Gauss-Bonnet theorem*, Phys. Rev. D **94** (2016) 084015, [arXiv:1604.08308](#).
- [68] Y. Chen, R. Roy, S. Vagnozzi, L. Visinelli, *Superradiant evolution of the shadow and photon ring of Sgr A**, Phys. Rev. D **106** (2022) 043021, [arXiv:2205.06238](#).
- [69] M. Afrin, S. Vagnozzi, S. G. Ghosh, *Tests of Loop Quantum Gravity from the Event Horizon Telescope Results of Sgr A**, Astrophys. J. **944** (2023) 149, [arXiv:2209.12584](#).
- [70] T. Q. Do, D. H. Nguyen, T. M. Pham, *Stability investigations of isotropic and anisotropic exponential inflation in the Starobinsky-Bel-Robinson gravity*, [arXiv:2303.17283](#).